Separation Science and Technology
Publication details, including instructions for authors and subscription information:
http://www.informaworld.com/smpp/title~content=t713708471

Countercurrent Extraction. Mass Transfer Kinetics and Time-Dependent Behavior

David J. Wilson[a]
[a] DEPARTMENT OF CHEMISTRY, VANDERBILT UNIVERSITY, NASHVILLE, TENNESSEE

To cite this Article Wilson, David J.(1988) 'Countercurrent Extraction. Mass Transfer Kinetics and Time-Dependent Behavior', Separation Science and Technology, 23: 1, 133 — 151

To link to this Article: DOI: 10.1080/01496398808057639

URL: http://dx.doi.org/10.1080/01496398808057639

SEPARATION SCIENCE AND TECHNOLOGY, 23(1-3), pp. 133-151, 1988

Countercurrent Extraction. Mass Transfer Kinetics and Time-Dependent Behavior

---

DAVID J. WILSON

DEPARTMENT OF CHEMISTRY
VANDERBILT UNIVERSITY
NASHVILLE, TENNESSEE 37235

Abstract

The time-dependent behavior of countercurrent extraction columns is modeled mathematically. The effects of aqueous and organic phase flow rates, number of theoretical plates, mass transfer kinetics, and pulse influent concentration overloads are determined. Use of an asymmetrical upwind algorithm to model advection allows substantial reductions in the computer time required. The effluent organic phase approaches its steady-state concentration much more rapidly than does the effluent aqueous phase.

INTRODUCTION

Solvent extraction techniques are widely used in analytical chemistry and in chemical technology; Dilts gives an excellent introduction to the subject and a good indication of the breadth of its applications (*1*). For industrial-scale applications, continuous countercurrent flow extraction is normally used. Analyses of countercurrent extractors operating in steady-state are given in a number of standard texts on chemical engineering (*2–5*). Analysis of countercurrent extractors provides techniques for handling other separation methods as well; we relied heavily on Wilburn's work (*6*) on countercurrent extraction in modeling the steady-state behavior of foam flotation columns (*7*), for example.

At times one is interested in the time-dependent behavior of a separation technique—the response of the device to a short-term shock loading, for instance. It is then necessary to model the behavior of the device by means of the time-dependent differential equations describing the evolution of the solute masses in the theoretical transfer units into which the column is partitioned. If the number of theoretical transfer units required to adequately represent the column is large (as in gas–liquid or liquid–liquid chromatography, for example), computer time and memory requirements become excessive. We have been able to reduce these requirements very substantially in the modeling of gas chromatography (*8*, *9*) and ion exchange (*10*, *11*) by the use of so-called asymmetrical upwind algorithms. Leonard (*12*, *13*) has utilized these very effectively in modeling advection terms with quite markedly reduced numerical dispersion, and has argued very persuasively for their use. The large number of theoretical transfer units required to model a high-resolution column is merely a reflection of the very high numerical dispersion associated with the algorithm used to represent advection in the theoretical plate model.

We here test one of the asymmetrical upwind algorithms for modeling advection in countercurrent extractors, and also use a time constant method for taking mass transport kinetics into account. The differential equations are well-adapted to exploring the response of countercurrent extraction columns to pulse overloads, and we investigate this by imposing square wave concentrations pulses on the column influent.

ANALYSIS

The analysis of countercurrent extraction breaks up into three fairly separate problems: 1) the determination of the countercurrent movement of the two phases in the column, 2) the estimation of the time constant for mass transfer between phases, and 3) the derivation and solution of the differential equations modeling the column. The partitioning of the column into compartments is shown schematically in Fig. 1.

First we consider the movements of the two liquid phases in the column. Let us focus on one compartment of radius R and thickness Δx. Notation is as follows.

Q_w = volumetric flow rate of aqueous phase, cm^3/s
Q_o = volumetric flow rate of organic phase, cm^3/s
r = radius of droplets of organic phase, cm
n = number of droplets introduced per second
v_o = velocity of droplets relative to the surrounding water, cm/s
v_o' = velocity of droplets relative to the laboratory, cm/s
v_w' = velocity of the aqueous phase relative to the laboratory, cm/s

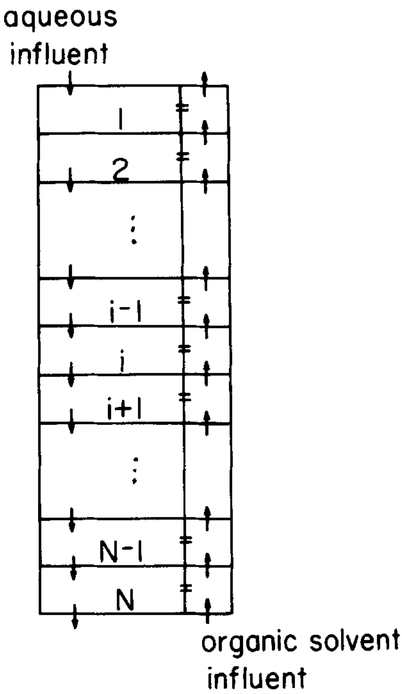

FIG. 1. The column model.

The number of droplets per unit length of column is given by $n\Delta x/v_o'$. Then the volume of organic liquid in one compartment is given by

$$V_o = n \cdot \frac{4\pi r^3}{3} \cdot \frac{\Delta x}{v_o'} = Q_o \frac{\Delta x}{v_o'} \tag{1}$$

From this we see that the volume of aqueous phase in one compartment is

$$V_w = \pi R^2 \Delta x - \frac{Q_o \Delta x}{v_o'} \tag{2}$$

and the volume of water per unit length of column is just

$$\frac{V_w}{\Delta x} = \pi R^2 - \frac{Q_o}{v_o} \tag{3}$$

where R = column radius, cm. The volumetric flow rate of the water is Q_w cm^3/s, so the linear velocity of the water relative to the laboratory is

$$v'_w = \frac{Q_w}{\pi R^2 - (Q_o/v'_o)} \tag{4}$$

Next, v_o, the droplet velocity relative to the surrounding water, is calculated iteratively from Eq. (5), which is obtained from a result given by Fair, Geyer, and Okun (*14*):

$$v_o = \frac{2(\Delta\rho)gr^2}{9\eta\left[1 + \frac{1}{4}\left(\frac{\rho_w r v_o}{2\eta}\right)^{1/2} + 0.34\,\frac{\rho_w r v_o}{12\eta}\right]} \tag{5}$$

where ρ_w = density of water, g/cm^3
ρ_o = density of organic liquid
$\Delta\rho = \rho_w - \rho_o$
η = viscosity of water, poise
g = 980 cm/s^2

The calculation is initialized by setting $v_o = 0$ on the RHS of Eq. (5); this gives Stokes' law.

The laboratory velocity of the droplets is given by

$$v'_o = v_o - v'_w \tag{6}$$

which on substitution from Eq. (4) yields

$$v'_o = v_o - \frac{Q_w}{\pi R^2 - Q_o/v'_o} \tag{7}$$

Rearrangement of this then yields a quadratic equation for v'_o,

$$\pi R^2(v'_o)^2 + (Q_w - Q_o - v_o\pi R^2)v'_o + Q_o v_o = 0 \tag{8}$$

for which the solutions are

$$v'_w = \frac{(Q_o + v_o\pi R^2 - Q_w) \pm \sqrt{(Q_o + v_o\pi R^2 - Q_w)^2 - 4\pi R^2 Q_o v_o}}{2\pi R^2} \tag{9}$$

If $Q_w = 0$, this yields

$$v_w' = \frac{Q_o + v_o\pi R^2 \pm (-Q_o + v_o\pi R^2)}{2\pi R^2} \tag{10}$$

(since Q_o is always $< v_o\pi R^2$). Since for this case we must have $v_o' = v_o$, we must select the positive sign in Eq. (9), so

$$v_w' = \frac{(Q_o + v_o\pi R^2 - Q_w) + \sqrt{(Q_o + v_o\pi R^2 - Q_w)^2 - 4\pi R^2 Q_o v_o}}{2\pi R^2} \tag{11}$$

Recall that the volume of organic phase in one compartment is given by

$$V_o = Q_o \Delta x / v_o' \tag{1'}$$

and the volume of aqueous phase in one compartment is

$$V_w = \pi R^2 \Delta x - V_o \tag{2'}$$

The contact time of an organic liquid droplet in one compartment is

$$\tau_o = \Delta x / v_o' \tag{12}$$

and the residence time of an element of water in a compartment is

$$\tau_w = \Delta x / v_w' \tag{13}$$

These relationships provide constraints on the size of Δt which can be used later in the numerical integration; Δt must be substantially less than the least of τ_o and τ_w.

This completes the analysis of the motions of the aqueous and organic phases. We now turn to the estimation of the time constant for mass transfer between the aqueous and organic phases. We shall include the effect of the quiescent boundary layer around the rising drop. Neglecting this boundary layer gives for the time constant for mass transfer

$$\tau = r^2/(\pi^2 D_o) \tag{14}$$

where D_o is the diffusion constant of the solute in the organic phase.

In this section alone let the droplet radius be a. Also let $b - a$ be the thickness of the quiescent boundary layer around the drop. Then the diffusion problem is as follows.

$$\frac{\partial c}{2t} = \frac{D_o}{r^2}\frac{\partial}{2r}\left(r^2\frac{\partial c}{2r}\right), \qquad 0 < r \leqslant a \text{ (Region I)} \tag{15}$$

$$\frac{\partial c}{2t} = \frac{D_w}{r^2}\frac{\partial}{2r}\left(r^2\frac{\partial c}{2r}\right), \qquad a < r \leqslant b \text{ (Region II)} \tag{16}$$

Here D_w is the solute diffusion constant in the aqueous phase. The boundary conditions are as follows.

$$c(0,t) \neq \infty \tag{17}$$

$$\lim_{\delta \to 0^+} c(\alpha - \delta,t) = \lim_{\delta \to 0^+} Kc(a + \delta,t) \tag{18}$$

We assume local equilibrium at the boundary between phases. K is the solute–water partition coefficient.

$$\lim_{\delta \to 0^+} D_o\frac{\partial c}{\partial r}(a - \delta,t) = \lim_{\delta \to 0^+} D_w\frac{\partial c}{\partial r}(a + \delta,t) \tag{19}$$

The flux of solute must be continuous at the boundary. Lastly

$$c(b,t) = c_\infty \tag{20}$$

where c_∞ is the bulk concentration of solute in the aqueous phase.

In Region I (the droplet) the solution to Eq. (15) is readily obtained by the substitution $u = c/r$ and then separating the variables; it is

$$c = \sum_\lambda \frac{A_\lambda}{r}\sin(\lambda D_o^{-1})^{1/2} r \exp(-\lambda t) + Kc_\infty \tag{21}$$

where we have already used Eq. (17) to eliminate all terms which are singular at $r = 0$.

In the aqueous boundary layer (Region II), the solution to Eq. (16) is

$$c(r,t) = \sum_\lambda \left[\frac{B_\lambda}{r}\cos(\lambda D_w^{-1})^{1/2} r + \frac{C_\lambda}{r}\sin(\lambda D_w^{-1}) r\right]\exp(-\lambda t) + c_\infty \tag{22}$$

The boundary conditions are now used. From Eq. (20),

$$B_\lambda \cos(\lambda D_w^{-1})^{1/2} b + C_\lambda \sin(\lambda D_w^{-1})^{1/2} b = 0 \tag{23}$$

From Eq. (18),

$$A_\lambda K^{-1} \sin(\lambda D_o^{-1})^{1/2}a - B_\lambda \cos(\lambda D_w^{-1})^{1/2}a - C_\lambda \sin(\lambda D_w^{-1})^{1/2}a = 0 \tag{24}$$

From Eq. (19), after some manipulation one obtains

$$\begin{aligned} &A_\lambda \frac{D_o}{D_w}\left[\sin \sqrt{\frac{\lambda}{D_o}}\,a - a\sqrt{\frac{\lambda}{D_o}} \cos \sqrt{\frac{\lambda}{D_o}}\,a\right] \\ &\quad + B_\lambda\left[-\cos \sqrt{\frac{\lambda}{D_w}}\,a - a\sqrt{\frac{\lambda}{D_w}} \sin \sqrt{\frac{\lambda}{D_w}}\,a\right] \\ &\quad + C_\lambda\left[-\sin \sqrt{\frac{\lambda}{D_w}}\,a + a\sqrt{\frac{\lambda}{D_w}} \cos \sqrt{\frac{\lambda}{D_w}}\,a\right] = 0 \end{aligned} \tag{25}$$

Equations (23), (24), and (25) are a set of three linear homogeneous equations in A_λ, B_λ, and C_λ. In order to obtain nonzero values for these constants, we must set the determinant of the coefficients in the equations equal to zero. This yields Eq. (26) (on page 140) as the eigenvalue equation which must be solved for this system. Zero is the lowest eigenvalue; our desired time constant is the reciprocal of the least positive eigenvalue, λ_1. λ_1 has as an upper bound the value $\pi^2 D_o/a^2$; the presence of a boundary layer cannot increase the value of λ_1 above its value in the absence of a boundary layer. Therefore

$$\tau > a^2/\pi^2 D_o \tag{27}$$

As a lower bound to λ_1 we may choose $\pi^2 D_{min}/b^2$, where D_{min} is the lesser of D_o and D_w. Since upper and lower bounds to λ_1 are known, it is possible to use either the regula falsi algorithm or a number of other search algorithms to find the desired root.

The analysis of column operation is as follows. We carry out the analysis using the theoretical plate model for advection for clarity; later this advection algorithm is replaced by one of the asymmetrical upwind algorithms to study the effect of these on numerical dispersion. The approach to be used is similar to one used to include mass transport kinetics in ion exchange and gas chromatography (*8–11*).

The rate of change of solute mass in the ith compartment is given by

$$dm_i/dt = Q_w(c_{i-1}^w - c_i^w) + Q_o(c_{i+1}^o - c_i^o) \tag{28}$$

To these equations we adjoin equations describing the changes in

$$\begin{vmatrix} \frac{D_o}{D_w}\left[\sin\sqrt{\frac{\lambda}{D_o}}\,a - a\sqrt{\frac{\lambda}{D_o}}\cos\sqrt{\frac{\lambda}{D_o}}\,a\right] & \left[-\cos\sqrt{\frac{\lambda}{D_w}}\,a - a\sqrt{\frac{\lambda}{D_w}}\sin\sqrt{\frac{\lambda}{D_w}}\,a\right] & \left[-\sin\sqrt{\frac{\lambda}{D_w}}\,a + a\sqrt{\frac{\lambda}{D_w}}\cos\sqrt{\frac{\lambda}{D_w}}\,a\right] \\ K^{-1}\sin\sqrt{\frac{\lambda}{D_o}}\,a & -\cos\sqrt{\frac{\lambda}{D_w}}\,a & -\sin\sqrt{\frac{\lambda}{D_w}}\,a \\ 0 & \cos\sqrt{\frac{\lambda}{D_w}}\,b & \sin\sqrt{\frac{\lambda}{D_w}}\,b \end{vmatrix} = 0 \qquad (26)$$

concentration in the two phases with the constraint that no mass transport takes place between the phases:

$$\frac{\delta c_i^w}{\delta t} = \frac{Q_w}{V_w}(c_{i-1}^w - c_i^w) \tag{29}$$

and

$$\frac{\delta c_i^o}{\delta t} = \frac{Q_o}{V_o}(c_{i+1}^o - c_i^o) \tag{30}$$

The assumption of Henry's law gives

$$c_{ei}^o = Kc_{ei}^w \tag{31}$$

where the subscript *e* indicates equilibrium. Mass balance gives

$$m_i = V_o c_{ei}^o + V_w c_{ei}^w \tag{32}$$

From these two equations we find

$$c_{ei}^w = \frac{m_i}{V_o K + V_w} \tag{33}$$

and

$$c_{ei}^o = \frac{Km_i}{V_o K + V_w} \tag{34}$$

One proceeds as follows. First, integrate Eqs. (28)-(30) forward one time increment Δt. This gives

$$m_i(t + \Delta t)$$

$$c_{0i}^w(t + \Delta t)$$

and

$$c_{0i}^o(t + \Delta t)$$

Then allow the concentrations to relax toward their equilibrium values via an exponential decay, yielding

$$c_i^w(t + \Delta t) = c_{0i}^w f + c_{ei}^w(1 - f) \qquad (35)$$

$$c_i^o(t + \Delta t) = c_{0i}^o f + c_{ei}^o(1 - f) \qquad (36)$$

where

$$f = \exp(-\Delta t/\tau) \qquad (37)$$

These, together with the $m_i(t + \Delta t)$, provide the initial conditions for the next integration step forward in time, so we repeat the cycle.

The boundary conditions at the ends of the column require separate treatment. At the top of the column

$$dm_1/dt = Q_w(c_{infl}^w - c_1^w) + Q_o(c_2^o - c_1^o) \qquad (38)$$

$$\frac{\delta c_1^w}{\delta t} = \frac{Q_w}{V_w}(c_{infl}^w - c_1^w) \qquad (39)$$

$$\frac{\delta c_1^o}{\delta t} = \frac{Q_o}{V_o}(c_2^o - c_1^o) \qquad (40)$$

At the bottom of the column

$$dm_N c_1^o/dt = Q_w(c_{N-1}^w - c_N^w) - Q_o c_N^o \qquad (41)$$

$$\frac{\delta c_N^w}{\delta t} = \frac{Q_w}{V_w}(c_{N-1}^w - c_N^w) \qquad (42)$$

$$\frac{\delta c_N^o}{\delta t} = -\frac{Q_o}{V_o} c_m^o \qquad (43)$$

This takes care of the boundary conditions.

If the axial dispersion of the column being modeled is small, requiring that N, the number of theoretical transfer units, be large, then the computer time and memory requirements can become excessive.

In this situation, use of one of the asymmetrical algorithms available for representing advection (*12*, *13*) results in great reduction in numerical dispersion, so that N can be reduced to a fourth or so of the value which would be necessary in the theoretical plate model. This, in turn, permits the use of larger values of Δt in the numerical integration. The resulting reductions in computer time and memory requirements make it feasible to run such jobs on a microcomputer. We note that "upwind" is in opposite directions for the organic and aqueous phases. We replace Eqs. (28), (29), and (30) by the following set of differential equations.

$$\frac{dm_i}{dt} = Q_w\left[-\frac{1}{8}c^w_{i-2} + \frac{7}{8}c^w_{i-1} - \frac{3}{8}c^w_i - \frac{3}{8}c^w_{i+1}\right]$$

$$+ Q_o\left[-\frac{1}{8}c^o_{i+2} + \frac{7}{8}c^o_{i+1} - \frac{3}{8}c^o_i - \frac{3}{8}c^o_{i-1}\right] \qquad (44)$$

$$\frac{\delta c^w_i}{\delta t} = \frac{Q_w}{V_w \Delta x}\left[-\frac{1}{8}c^w_{i-2} + \frac{7}{8}c^w_{i-1} - \frac{3}{8}c^w_i - \frac{3}{8}c^w_{i+1}\right] \qquad (45)$$

$$\frac{\delta c^o_i}{\delta t} = \frac{Q_o}{V_o \Delta x}\left[-\frac{1}{8}c^o_{i+2} + \frac{7}{8}c^o_{i+1} - \frac{3}{8}c^o_i - \frac{3}{8}c^o_{i-1}\right] \qquad (46)$$

Notice the reversal in order in the terms associated with the movement of the organic phase, which is flowing countercurrent to the aqueous phase. These equations require modification at the top and bottom of the column, since they require nonexistent values of the concentration at these boundaries.

The following equations are used at the top and bottom of the column to avoid this problem. At the top,

$$\frac{\delta c^w_1}{\delta t} = \frac{Q_w}{V_w \Delta x}(c_{infl} - c^w_1) \qquad (47)$$

$$\frac{\delta c^w_2}{\delta t} = \frac{Q_w}{V_w \Delta x} = \left(\frac{9}{8}c^w_1 - \frac{3}{4}c^w_2 - \frac{3}{8}c^w_3\right) \qquad (48)$$

$$\frac{\delta c^o_1}{\delta t} = \frac{Q_o}{V_o \Delta x}\left(-\frac{1}{8}c^o_3 + \frac{3}{4}c^o_2 - \frac{5}{8}c^o_1\right) \qquad (49)$$

$$\frac{\delta c^o_2}{\delta t} = \frac{Q_o}{V_o \Delta x}\left(-\frac{1}{8}c^o_4 + \frac{7}{8}c^o_3 - \frac{3}{8}c^o_2 - \frac{3}{8}c^o_1\right) \qquad (50)$$

$$\frac{dm_1}{dt} = V_w \Delta x \frac{\delta c^w_1}{\delta t} + V_o \Delta x \frac{\delta c^o_1}{\delta t} \qquad (51)$$

$$\frac{dm_2}{dt} = V_w \Delta x \frac{\delta c^w_2}{\delta t} + V_o \Delta x \frac{\delta c^o_2}{\delta t} \qquad (52)$$

At the bottom of the column,

$$\frac{\delta c_N^w}{\delta t} = \frac{Q_w}{V_w \Delta x}\left(-\frac{1}{8}c_{N-2}^w + \frac{3}{4}c_{N-1}^w - \frac{5}{8}c_N^w\right) \tag{53}$$

$$\frac{\delta c_{N-1}^w}{\delta t} = \frac{Q_w}{V_w \Delta x}\left(-\frac{1}{8}c_{N-3}^w + \frac{7}{8}c_{N-2}^w - \frac{3}{8}c_{N-1}^w - \frac{3}{8}c_N^w\right) \tag{54}$$

$$\frac{\delta c_N^o}{\delta t} = \frac{Q_o}{V_o \Delta x}(-c_N^o) \tag{55}$$

$$\frac{\delta c_{N-1}^o}{\delta t} = \frac{Q_o}{V_o \Delta x}\left(\frac{9}{8}c_N^o - \frac{3}{4}c_{N-1}^o - \frac{3}{8}c_{N-2}^o\right) \tag{56}$$

$$\frac{dm_N}{dt} = V_w \Delta x \frac{\delta c_N^w}{\delta t} + V_o \Delta x \frac{\delta c_N^o}{\delta t} \tag{57}$$

$$\frac{dm_{N-1}}{dt} = V_w \Delta x \frac{\delta c_{N-1}^w}{\delta t} + V_o \Delta x \frac{\delta c_{N-1}^o}{\delta t} \tag{58}$$

The rather substantial axial dispersion in most countercurrent extraction columns probably makes these refinements unnecessary in normal use.

RESULTS AND CONCLUSIONS

The models described were programmed in BASICA, and compiled and run on a Zenith 150 microcomputer running at 4.77 MHz. A typical run of 5000 s with the column partitioned into 10 compartments required about 130 min. A listing of standard values for the model parameters is given in Table 1; departures from these values are given in the captions to the figures.

In Fig. 2 we see the approach of the column to a steady-state from an initial state in which no solute is present in the column. It is apparent that, for flow rates of the organic solvent less than 1.0 mL/s, this column is overloaded. In all of the runs the organic effluent approaches its steady-state concentration much more quickly than the aqueous effluent approaches its steady-state concentration. Since the linear velocity of the organic phase is 2.9 cm/s, while that of the aqueous phase is only 0.20 cm/s, this result is hardly surprising.

TABLE 1
Standard Values of the Parameters Used in the Model

Water density	1.00 g/mL
Organic solvent density (toluene)	0.8669 g/mL
Viscosity of water	0.01119 poise
Organic solvent drop diameter	0.1 cm
Flow rate of aqueous phase	10 mL/s
Column radius	4 cm
Column height	100 cm
Number of compartments into which the column is partitioned	10
Mass transfer time constant	0.01 s
Influent concentration	0.8 g/mL
Distribution coefficient	10
Δt	0.25 s
b (0 = theoretical plate, 1 = asymmetrical upwind)	0

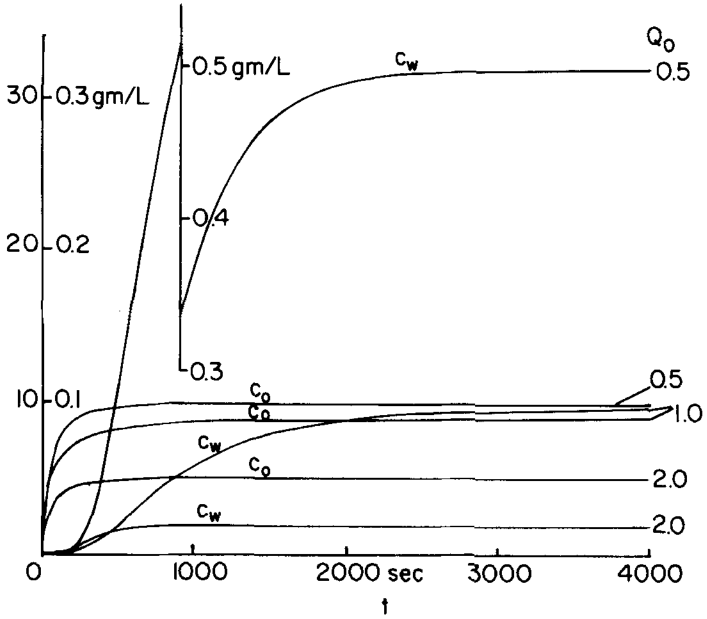

FIG. 2. Effluent aqueous and organic phase solute concentrations as functions of time. Organic phase flow rates = 0.5, 1.0, and 2.0 mL/s. Note displacement of the vertical axis for Q_o = 0.5 mL/s. The left scale on the ordinate (from 0 to 0.3, or 0.3 to 0.5) refers to the concentration in the aqueous phase, c^w. Parameters not given here are as in Table 1.

The effect of Δt on the steady-state removal efficiencies is shown in Fig. 3. The lower line shows removal efficiency as calculated from the aqueous effluent concentration; the upper, removal efficiency as calculated from the organic phase effluent concentration. We selected $\Delta t = 0.25$ s as a reasonable compromise between speed and accuracy.

The data plotted in Fig. 4 show the relationship between removal and organic solvent flow rate (Q_o) in more detail than was possible in Fig. 2. For the parameters selected here, a value of Q_o of about 1.0 mL/s marks the boundary between poor removal efficiency ($Q_o < 1$ mL/s) and good removal efficiency ($Q_o > 1$ mL/s).

The effect of axial dispersion (or, equivalently, number of theoretical plates) is seen in Fig. 5. With the system being modeled there is little incentive to try to achieve more than 10–15 theoretical transfer units unless one is striving for removal efficiencies extremely close to 100%. It is also evident that separation efficiencies decrease markedly as N decreases below about 7; such columns should be baffled and/or the distribution head for the organic phase redesigned to increase the value of N.

The size of the mass transfer time constant τ has a substantial effect on removal efficiency, as exhibited in Fig. 6. The fall-off in removal efficiency becomes large when τ is of roughly the same size as the time required for a droplet of organic phase to move from the bottom of the column to its top.

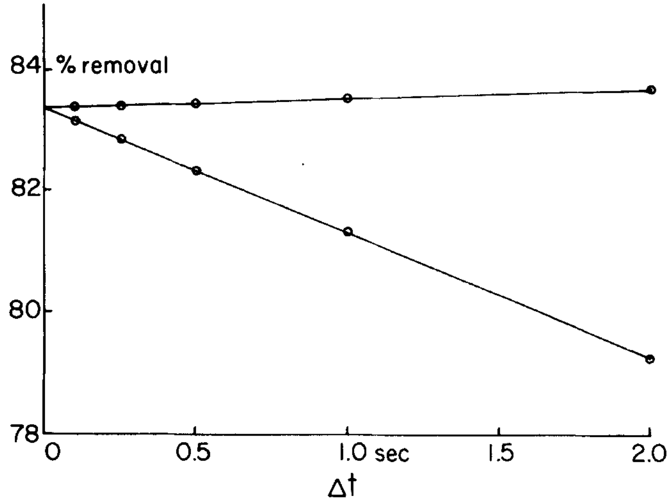

FIG. 3. Effect of Δt on the % removal as measured by the concentrations in the organic effluent (upper line) and in the aqueous effluent (lower line). $Q_o = 1.0$ mL/s.

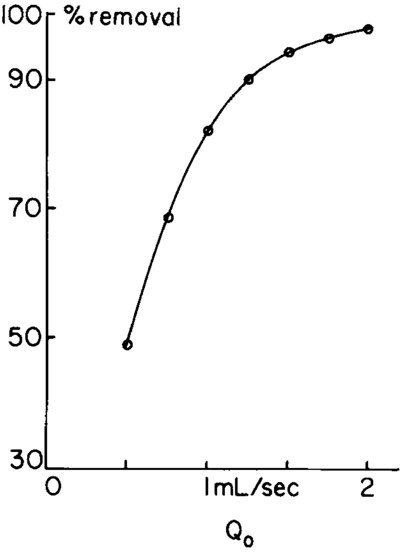

FIG. 4. Effect of organic phase flow rate on removal efficiency.

The effects of concentration pulses are seen in Figs. 7 and 8. In Fig. 7 the plots are generated by square-wave concentration pulses of 1.5, 2.0, and 2.5 g/L in the influent between $t = 1000$ and 2000 s. The baseline influent concentration is 0.8 g/L. The solute concentration in the organic phase effluent responds much more quickly to variations in the influent

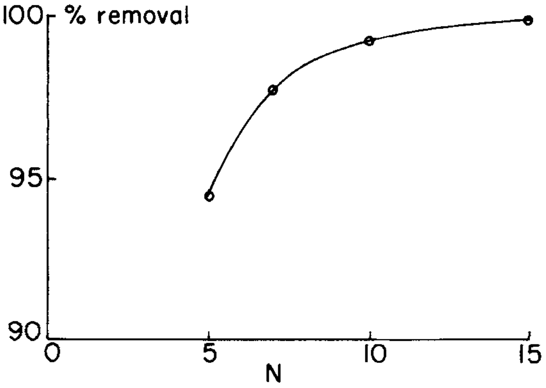

FIG. 5. Effect of the number of theoretical plates on the removal efficiency. Q_o = 1.5 mL/s.

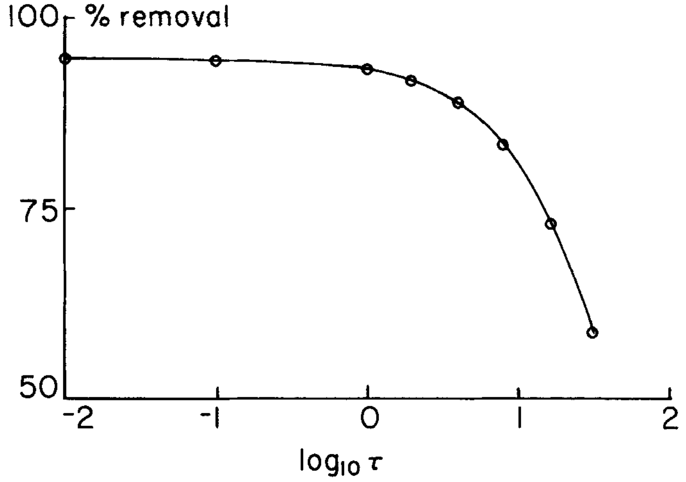

FIG. 6. Effect of mass transfer time constant τ (s) on removal efficiency. Q_o = 1.5 mL/s.

concentration than does the aqueous effluent concentration, in agreement with the results shown in Fig. 2. In Fig. 8 the plots are generated by square wave influent concentration pulses of 2.0 g/L beginning at t = 1000 s and continuing to 1500, 2000, and 2500 s. In all of the runs in Figs. 7 and 8 the column was initially charged with an aqueous phase containing 0.8 g/L of solute.

The asymmetrical upwind algorithm can represent columns of higher efficiency for a given value of N than can the theoretical plate algorithm, as seen in Table 2. This shows up particularly spectacularly at a flow rate Q_o of 1.0 mL/s, where the aqueous effluent concentration for $b = 1$ (asymmetrical upwind) is about a tenth as large as the aqueous effluent concentration for $b = 0$ (theoretical plate). If one is attempting to model columns with very low axial dispersion, use of an asymmetrical upwind algorithm for modeling should result in substantial savings of computer time.

We conclude that 1) modeling the time-dependent operation of countercurrent extraction columns on microcomputers is quite feasible, 2) a time constant approach to mass transfer kinetics is easily carried out, and 3) the use of an asymmetrical upwind algorithm for modeling advective transport in columns having low axial dispersion can greatly reduce the computer time required. A diskette for MS-DOS computers with the BASIC A source program and the compiled program is available from the author for $3.00 to cover the costs of mailing and the diskette.

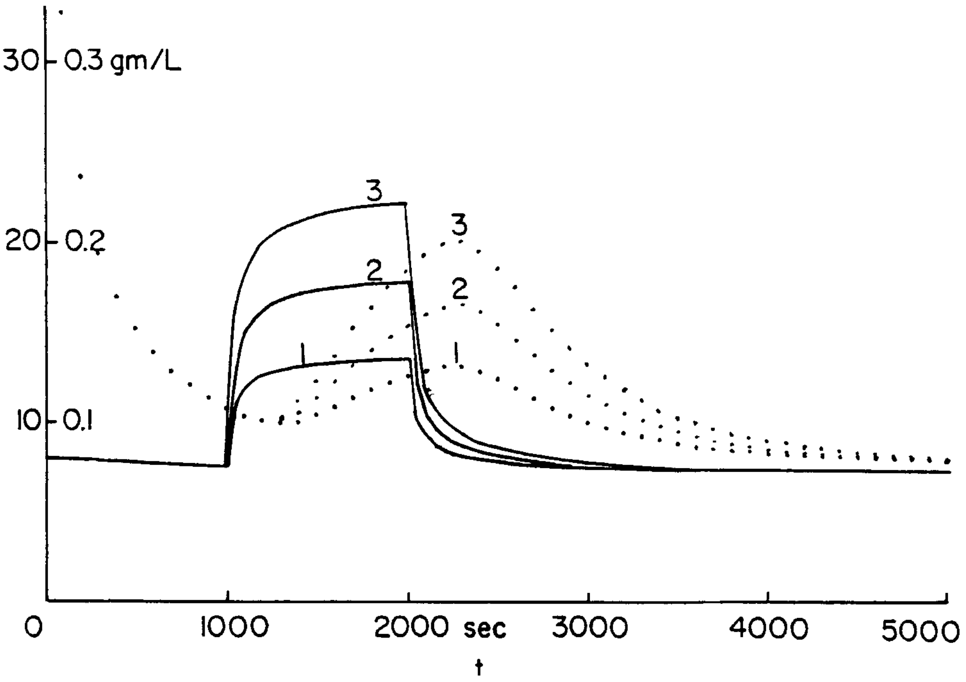

FIG. 7. Effect of an influent concentration pulse on column behavior. The background value for c_{infl} is 0.8 g/L. The square pulse concentration values are 1.5 (1), 2.0 (2), and 2.5 (3) g/L, and the pulses last from $t = 1000$ to $t = 2000$ s. The two scales on the ordinate refer to c^o_{effl} (0 to 30) and c^w_{effl} (0 to 0.3). $Q_o = 1.0$ mL/s.

TABLE 2
Effect of Asymmetrical Upwind Algorithm in Increasing Column Efficiency at Constant N^a

	Efficiency (%)	
Q_o (mL/s)	$b = 0$	$b = 1$
0.5	49.01	50.10
1.0	82.33	98.28
2.0	98.07	99.999

$^a N = 10$, $Q_w = 10$ mL/s, $c_{\mathit{infl}} = 0.8$ g/mL, $\Delta t = 0.25$ s in all runs.

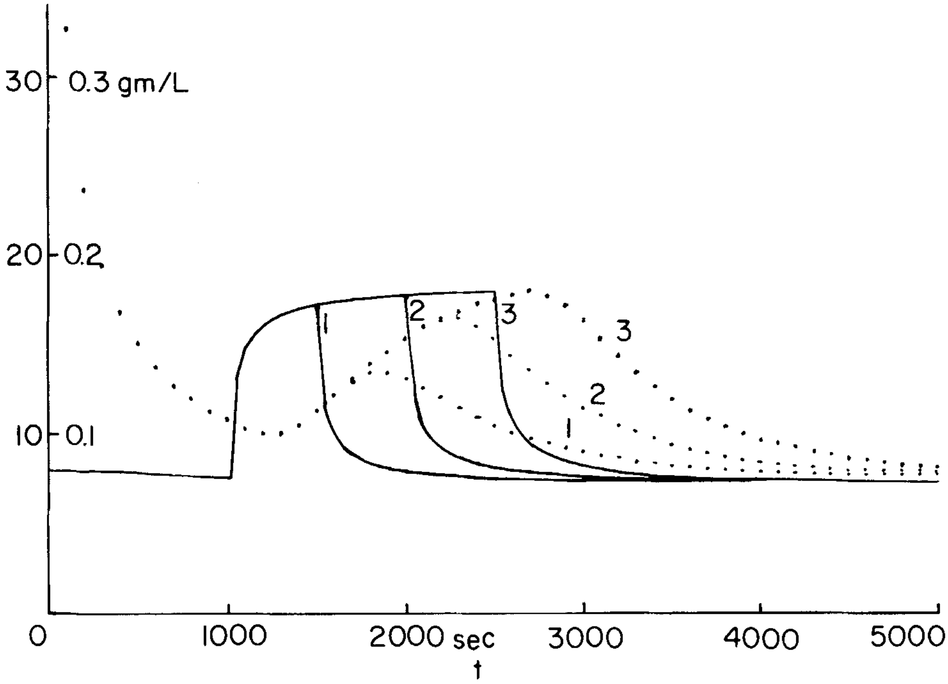

FIG. 8. Effect of concentration pulse duration on column behavior. The background value for c_{infl} is 0.8 g/L. The square pulse concentration values are 2.0 g/mL, and the pulses last from 1000 to 1500 (1), 2000 (2), and 3000 (3) s. The two scales on the ordinate are as defined in Fig. 7. Q_0 = 1.0 mL/s.

Acknowledgment

This work was supported by a grant from the National Science Foundation.

REFERENCES

1. R. V. Dilts, *Analytical Chemistry*, Van Nostrand, New York, 1974, Chap. 6.
2. R. E. Treybal, *Mass-Transfer Operations*, 2nd ed., McGraw-Hill, New York, 1968, Chap. 10.
3. C. D. Holland, *Fundamentals and Modeling of Separation Processes*, Prentice-Hall, Englewood Cliffs, New Jersey, 1975, Chap. 5 and 12.
4. H. Freiser, B. L. Karger, L. R. Snyder, and C. Horvath (eds.), *An Introduction to Separation Science*, Wiley-Interscience, New York, 1973.
5. W. L. McCabe and J. C. Smith, *Unit Operations of Chemical Engineering*, 2nd ed., McGraw-Hill, New York, 1967.

6. N. P. Wilburn, *Ind. Eng. Chem., Fundam., 3,* 189 (1964).
7. J. W. Wilson, D. J. Wilson, and J. H. Clarke, *Sep. Sci., 11,* 223 (1976).
8. D. J. Wilson, *Sep. Sci. Technol., 21,* 887 (1986).
9. D. J. Wilson, *Ibid., 22,* 1835 (1987).
10. D. J. Wilson, *Ibid., 21,* 767 (1986).
11. D. J. Wilson, *Ibid., 21,* 991 (1986).
12. B. P. Leonard, *Comput. Methods Appl. Mech. Eng., 19,* 59 (1979).
13. B. P. Leonard, in *Finite Element Methods for Convection Dominated Flows* (T. J. R. Hughes, ed.), American Society of Mechanical Engineers, New York, 1979.
14. G. M. Fair, J. C. Geyer, and D. A. Okun, *Water and Wastewater Engineering. Vol. II. Wastewater Treatment and Disposal,* Wiley, New York, 1968, Section 25-2.
15. C. D. Hodgman, *Handbook of Chemistry and Physics,* 42nd ed., Chemical Rubber Publishing Co., Cleveland, Ohio, 1960.

Received by editor April 22, 1987